applied sciences

MDPI

Article

Polymerization of Isobutylene in a Rotating Packed Bed Reactor: Experimental and Modeling Studies

Wenhui Hou [1,2], Wei Wang [3], Yang Xiang [2], Yingjiao Li [1,2], Guangwen Chu [1,2], Haikui Zou [2,*] and Baochang Sun [2,*]

[1] State Key Laboratory of Organic-Inorganic Composites, Beijing University of Chemical Technology, Beijing 100029, China; houwenhui2020@163.com (W.H.); 2020400015@mail.buct.edu.cn (Y.L.); chugw@mail.buct.edu.cn (G.C.)
[2] Research Center of the Ministry of Education for High Gravity Engineering and Technology, Beijing University of Chemical Technology, Beijing 100029, China; xiangy@mail.buct.edu.cn
[3] Beijing Water Business Doctor Co., Ltd., Beijing 100875, China; a18272632432@163.com
* Correspondence: zouhk@mail.buct.edu.cn (H.Z.); sunbc@mail.buct.edu.cn (B.S.); Tel.: +86-10-64443134 (B.S.)

Abstract: Polymerization of isobutylene (IB) for synthesizing highly reactive polyisobutylene (HRPIB) is characterized by a complicated fast intrinsic reaction rate; therefore, the features of its products exhibit a strong dependence on mixing efficiency. To provide uniform and efficient mixing, a rotating packed bed was employed as a reactor for polymerization of IB. The effects of operating parameters including polymerization temperature (T), rotating speed (N) and relative dosage of monomers and initiating systems ($[M]_0/[I]_0$) on number-average molecular weight (M_n) of HRPIB were studied. HRPIB with M_n of 2550 g·mol^{-1} and exo-olefin terminal content of 85 mol% were efficiently obtained at suitable conditions as T of 283 K, N of 1600 rpm and $[M]_0/[I]_0$ of 49. Moreover, the M_n can be regulated by changing T, N and $[M]_0/[I]_0$. Based on the presumptive-steady-state analysis method and the coalescence–redispersion model, a model for prediction of the M_n was developed and validated, and the calculated M_n values agreed well with experimental results, with a deviation of ±10%. The results demonstrate that RPB is a promising reactor for synthesizing HRPIB, and the given model for M_n can be applied for the design of RPB and process optimization.

Keywords: polymerization of isobutylene; highly reactive polyisobutylene; rotating packed bed; modeling

check for updates

Citation: Hou, W.; Wang, W.; Xiang, Y.; Li, Y.; Chu, G.; Zou, H.; Sun, B. Polymerization of Isobutylene in a Rotating Packed Bed Reactor: Experimental and Modeling Studies. *Appl. Sci.* **2021**, *11*, 10194. https://doi.org/10.3390/app112110194

Academic Editor: Carolina Belver

Received: 23 September 2021
Accepted: 27 October 2021
Published: 30 October 2021

Publisher's Note: MDPI stays neutral with regard to jurisdictional claims in published maps and institutional affiliations.

Copyright: © 2021 by the authors. Licensee MDPI, Basel, Switzerland. This article is an open access article distributed under the terms and conditions of the Creative Commons Attribution (CC BY) license (https://creativecommons.org/licenses/by/4.0/).

1. Introduction

Polyisobutylene (PIB), the product of isobutylene (IB) polymerization, is an important organic polymer with excellent low gas permeability and high chemical stability, and it can be applied in many fields, such as oil additives, adhesive agents, sealants, paint and lubricants [1]. According to molecular weight, the PIB can be classified as low molecular weight PIB (M_n < 5000 g·mol^{-1}), medium molecular weight PIB (40,000 g·mol^{-1} < M_n < 100,000 g·mol^{-1}) and high molecular weight PIB (M_n > 100,000 g·mol^{-1}) [2]. Low molecular weight polyisobutylene with external olefin terminal group accounts for about 75% of the polyethylene market due to its substantial use as a precursor for the preparation of less dispersive agents [2]. In the last fifteen years, the three major methods for synthesizing highly reactive polyisobutylene (HRPIB) have been proposed in several articles: (i) using an active cation polymerization technique [3,4], (ii) using the Lewis acid complex as a catalyst [3,4] and (iii) using a solvent with weak coordination countra-ions to link metal complexes [5,6]. It has been reported that HRPIB with low molecular weights can be directly synthetized by cationic polymerization of IB with initiating systems of $H_2O/AlCl_3$/dialklyl ether and $H_2O/FeCl_3$/dialkyl ether [1,7], which is quite promising for the synthesis of HRPIB.

In the process of synthesizing HRPIB by the cationic polymerization of IB, one of the most important and difficult problems is the selection of reactors. The difficulty lies in that the rate constants of propagation in the cationic polymerization of alkenes are similar for most systems with $k_p = 10^{5\pm1}$ L·mol^{-1}·s^{-1} [8,9], which means that the cationic

polymerization of IB is featured with an extremely fast intrinsic reaction rate. The apparent reaction rate would be significantly affected by micromixing [10–14]. The extremely rapid polymerization needs reactors that can provide uniform mixing with high efficiency because the properties of the products are greatly affected by the mixing process. Poor and slow mixing of monomers and initiating agents results in inferior products [13,15,16]. More specifically, a principle for the selection of ideal cationic polymerization reactors is proposed as $t_m \leq t_{1/2}$ by Chen et al. [17], where t_m is micromixing characteristic time for the species to reach a maximum mixed state at the molecule level and $t_{1/2}$ is reactive characteristic time. The $t_{1/2}$ of the cationic polymerization with k_p of $10^{5\pm1}$ L·mol^{-1}·s^{-1} is estimated in the range of 0.01 to 0.1 ms, while the t_m of a typical stirred tank reactor is estimated in the region of 5 to 50 ms [18]. Therefore, traditional stirred tanks are not ideal reactors for the polymerization of IB.

As an apparatus for achieving high gravity conditions on the earth, a rotating packed bed (RPB) reactor mainly consists of a packed rotator and a fixed casing. The high gravity environment is produced by the centrifugal force created by the fast-spinning packed rotator. In RPB, the fluids going through the packing are split into very fine droplets, threads and thin films by the strong shear force, providing a sizeable and fast phase contact area, and resulting in a significant intensification of mixing and mass transfer between the fluid elements [19–21]. The rate of the mass transfer between gas and liquid in RPB is one to three orders of magnitude larger than that in a conventional packed bed reactor [22–27]. Notably, the value of t_m in RPB is estimated as 0.01 to 0.1 ms [28], which corresponds to the $t_{1/2}$ of the cationic polymerization. In terms of these unique features, RPB has been successfully applied to efficiently obtain butyl rubber with M_n of 289,000 g·mol^{-1} via cationic copolymerization of isobutylene and isoprene, and the production capacity per unit equipment volume increases by two to three orders of magnitude [17,29]. Therefore, it can be deduced that a comprehensive study of the polymerization of IB in RPB is prospective.

Based on the above considerations, the polymerization of IB in RPB was carried out for the first time. Operating parameters including polymerization temperature (T), rotating speed of the rotator (N) in RPB and relative dosage of monomers and initiating systems were studied to investigate their effects on the M_n of HRPIB. A theoretical model for prediction of M_n was also developed, and the theoretical values were compared with the experimental values.

2. Materials and Methods

2.1. Reagents

Isobutylene (polymer grade, purity > 99%, Beijing Yanshan Petrochemical Group, Beijing, China) was used as the main reactant. The $H_2O/AlCl_3$/dialklyl ether system described by Liu et al. [7] was used as the initiating system for the polymerization of IB and kindly supplied by Liu's lab. Dichloromethane (purity > 99.5%, Beijing Yili Fine Chemical Co., Beijing, China) was used as a solvent for the monomers and the initiating system, and it was distilled before using. Alcohol was used to terminate the polymerization. Tetrahydrofuran (purity > 99.5%, Beijing Yili Fine Chemical Co., China) was used for testing.

2.2. Experimental Procedures

The experimental set-up for the polymerization of IB in RPB is shown schematically in Figure 1. The used RPB is mainly composed of a packed rotator, a fixed casing, a distributor with two liquid inlets, a liquid outlet and a jacket for coolant. The inner and outer diameters of the rotator are 80 mm and 152 mm, respectively, and the axial width of the packing part is 42 mm. The rotating speed of the rotator can be changed from 0 to 2850 rpm.

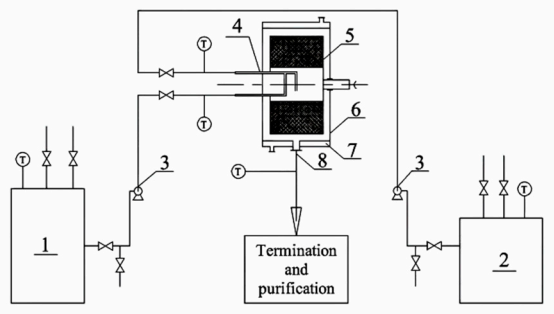


Figure 1. Schematic diagram of the experimental set-up for the polymerization of IB in RPB: 1—a tank for the solution of IB, 2—a tank for the solution of the initiating system, 3—metering pumps, 4—liquid inlets and distributors, 5—the packed rotator, 6—the fixed casing, 7—the jacket for coolant, 8-the liquid outlet.

All pipelines and equipment in Figure 1 were washed by dichloromethane and swept by nitrogen before using. The dichloromethane solution of IB and the initiating system were stored in tank 1 and tank 2 and refrigerated to a certain temperature with magnetic stirring. Concentrations of IB and the initiating system were expressed by $[M]_t$ and $[I]_t$, respectively. RPB was refrigerated to a certain temperature by cycling the coolant in the jacket of RPB. The solution of IB and the initiating system were separately pumped into RPB with volumetric flow rates of Q_M and Q_I, respectively, then premixed and distributed to the packing by the distributors. Q_M and Q_I were controlled by metering pumps. The mixing and polymerization of the reactants occurred in RPB and were terminated by alcohol at the liquid outlet of RPB. Operating parameters including T, $[M]_t$, $[I]_t$, Q_M, Q_I and N were gradually changed to obtain their effects on the M_n of the products.

The molecular weight (M_n) of the polymerization products was determined by the Waters 5151–2410 GPC instrument equipped with three Styragel GPC columns (HT3, HT5 and HT6E). Tetrahydrofuran was used as mobile phase, PS was used as standard sample curve and the volumetric flow rate was 1.0 mL/min at 30 °C. The molecular structure of the polymer, especially the exo-olefin terminal content, was determined by ^{1}H-NMR spectroscopy of the polymer solution in $CDCl_3$ with a Bruker spectrometer (400 MHz) at 25 °C [7], with tetramethylsilane as the standard reference.

2.3. Model Development

Based on a coalescence–redispersion model [30], which was successfully used to describe the micromixing in RPB, a chain analysis method was used to develop a mathematical model for simulating the cationic polymerization process in RPB and predicting the M_n of IIR as a function of T, N and D [31]. Analogously, this work tried to develop a new mathematical model, which combines the presumptive-steady-state analysis method and the coalescence–redispersion model [16,31].

2.3.1. Modeling for the Polymerization of IB in RPB

The assumptions of the coalescence–redispersion model, including the packing of RPB, liquid flow in the packing, coalescence–redispersion of droplets on cages, polymerization between two adjacent cages and estimation of droplet parameters and residence time are imitated in the model of this work [17]. The parameter values used in this study are given in Table 1.

Table 1. Parameter values of RPB used in the model.

N_D	N_L	δ/mm	R_i/mm	R_o/mm
600	40	0.9	40	76

2.3.2. Presumptive-Steady-State Analysis for the Polymerization

The monomer is denoted by M, the initiator is denoted by I, the solvent is denoted by S and the polymer with j units and active center is denoted by P_j. The polymerization mechanism and the reaction rate are expressed by Equations (1)–(5). Chain transfer reactions are mainly the transfer of active chains to chain transfer agents, monomers and solvents [32]. Transfer of active chain to chain transfer agent was not involved in this study. Transfer of active chain to monomer is shown in Equation (3), and transfer of active chain to solvent, including ether-assisted chain transfer reaction, is shown in Equation (4). On the basis of reactions (1)–(5), the reaction rate of M can be determined by Equation (6).

Initiation:

$$\mathrm{I} + \mathrm{M} \xrightarrow{k_i} \mathrm{P}_1^{\oplus}\mathrm{B}^{\ominus};\ r_i = k_i[\mathrm{I}][\mathrm{M}] \tag{1}$$

Propagation:

$$\mathrm{P}_1^{\oplus} + \mathrm{M} \xrightarrow{k_P} \mathrm{P}_{j+1}^{\oplus}\mathrm{B}^{\ominus};\ r_{P,M} = k_P\left[\mathrm{P}^{\oplus}\right][\mathrm{M}] \tag{2}$$

Transfer to the monomer:

$$\mathrm{P}_j^{\oplus}\mathrm{B}^{\ominus} + \mathrm{M} \xrightarrow{k_{tr,1}} \mathrm{P}_j + \mathrm{P}_1^{\oplus}\mathrm{B}^{\ominus};\ r_{tr,M} = k_{tr,1}\left[\mathrm{P}^{\oplus}\right][\mathrm{M}] \tag{3}$$

Transfer to the solvent:

$$\mathrm{P}_j^{\oplus}\mathrm{B}^{\ominus} + \mathrm{S} \xrightarrow{k_{tr,2}} \mathrm{P}_j + \mathrm{S}^{\oplus}\mathrm{B}^{\ominus};\ \mathrm{r}_{\mathrm{tr,S}} = k_{tr,2}\left[\mathrm{P}^{\oplus}\right][\mathrm{S}] \tag{4}$$

Termination:

$$\mathrm{P}_j^{\oplus}\mathrm{B}^{\ominus} \xrightarrow{k_t} \mathrm{P}_j;\ r_t = k_t\left[\mathrm{P}^{\oplus}\right] \tag{5}$$

$$r_M = -\frac{\mathrm{d}[\mathrm{M}]}{\mathrm{dt}} = k_P\left[\mathrm{P}^{\oplus}\right][\mathrm{M}] + k_{tr,1}\left[\mathrm{P}^{\oplus}\right][\mathrm{M}] + k_i[\mathrm{I}][\mathrm{M}] \tag{6}$$

For the presumptive-steady-state analysis method, the concentration of the active center $P_j^{\oplus}$ can be approximately regarded as a constant when the polymerization is in the stable state, because the polymerization of IB proceeded in an open system. This is to say $r_i = r_t$, and then,

$$-\frac{\mathrm{d}[\mathrm{p}^{\oplus}]}{\mathrm{dt}} = k_i[\mathrm{I}][\mathrm{M}] - k_t\left[\mathrm{p}^{\oplus}\right] = 0, \text{ and } \left[\mathrm{p}^{\oplus}\right] = \frac{k_i[\mathrm{I}][\mathrm{M}]}{k_t} \tag{7}$$

$$r_M = -\frac{\mathrm{d}[\mathrm{M}]}{\mathrm{dt}} = k_{tr,1}\frac{k_i[\mathrm{I}][\mathrm{M}]}{k_t}[\mathrm{M}] + k_i[\mathrm{I}][\mathrm{M}] + k_P\frac{k_i[\mathrm{I}][\mathrm{M}]}{k_t}[\mathrm{M}] \tag{8}$$

Compared with the propagation process, initiation and transfer can be ignored when the polymerization is in the stable state and a polymer with high M_n is continuously generated. Equation (8) is simplified as Equation (9). A simplification similar to Equations (6)–(9) is carried out from Equations (10)–(13). The consumption rate of I can be described as Equation (14).

$$r_M = -\frac{\mathrm{d}[\mathrm{M}]}{\mathrm{dt}} = \frac{k_i k_P}{k_t}[\mathrm{I}][\mathrm{M}]^2, \text{ or } \frac{\mathrm{d}[\mathrm{M}]}{\mathrm{dt}} = -\frac{k_i k_P}{k_t}[\mathrm{I}][\mathrm{M}]^2 \tag{9}$$

$$-\frac{\mathrm{d}\left[\mathrm{P_j}\right]}{\mathrm{dt}} = (k_t + k_{tr,1}[\mathrm{M}] + k_{tr,2}[\mathrm{S}])[\mathrm{P}_j^{\oplus}] \tag{10}$$

$$-\frac{\mathrm{d}\left[\mathrm{p}_1^{\oplus}\right]}{\mathrm{dt}} = k_p\left[\mathrm{p}_{j-1}^{\oplus}\right][\mathrm{M}] - k_p\left[\mathrm{p}_j^{\oplus}\right][\mathrm{M}] - k_{tr,1}\left[\mathrm{p}_j^{\oplus}\right][\mathrm{M}] - k_{tr,2}\left[\mathrm{p}_j^{\oplus}\right][\mathrm{S}] - k_t\left[\mathrm{p}_j^{\oplus}\right] = 0,$$

$$\text{and } [P_j^{\oplus}] = \frac{k_P[\mathrm{M}]}{k_P[\mathrm{M}] + k_t + k_{tr,1}[\mathrm{M}] + k_{tr,2}[\mathrm{S}]}[\mathrm{P}_{j-1}^{\oplus}] = \left\{\frac{k_P[\mathrm{M}]}{k_P[\mathrm{M}] + k_t + k_{tr,1}[\mathrm{M}] + k_{tr,2}[\mathrm{S}]}\right\}^{j-1}[\mathrm{P}_1^{\oplus}] \tag{11}$$

$$\frac{d[P_1^{\oplus}]}{dt} = k_i[I][M] - k_p[p_1^{\oplus}][M] - k_t[p_1^{\oplus}] + k_{tr,1}[P^{\oplus}][M] - k_{tr,1}[P_1^{\oplus}][M] + k_{tr,2}[P^{\oplus}][S] - k_{tr,2}[P_1^{\oplus}][S] = 0$$

$$\text{and } [P_1^{\oplus}] = \frac{k_i[I][M] + k_{tr,1}[M]\frac{k_i[I][M]}{k_t} + k_{tr,2}[S]\frac{k_i[I][M]}{k_t}}{k_p[M] + k_t + k_{tr,1}[M] + k_{tr,2}[S]} \quad (12)$$

$$\frac{d[P_j]}{dt} = \frac{(k_i[I][M]+1)(k_t + k_{tr,1}[M] + k_{tr,2}[S])}{k_P[M] + k_t + k_{tr,1}[M] + k_{tr,2}[S]} \left(\frac{k_P[M]}{k_P[M] + k_t + k_{tr,1}[M] + k_{tr,2}[S]}\right)^{j-1} \quad (13)$$

$$\frac{d[I]}{dt} = -k_i[I][M] \quad (14)$$

2.3.3. Calculation of M_n

On the basis of the coalescence–redispersion model in RPB, the concentrations of M, P_j and I can be calculated by solving Equations (9), (13) and (14). The simulation flow chart is shown in Figure 2, where the Monte Carlo random functions are adopted to characterize the coalescence–redispersion of the liquid through the packing, and the Runge–Kutta numerical method was adopted to solve the concentration of every structural unit [17,33,34]. Through the calculation on cages 1 to N_L, $[P_j]_{N_{L,\,out}}$ in each droplet can be obtained, and the average concentration of P_j is calculated by Equation (15). Then, the number-average molecule weight out of the packing can be theoretically predicted by Equation (16). With different initial conditions, different M_n can be calculated and the effect of polymerization parameters on M_n can be analyzed.

$$\overline{[P_j]_{N_{L,\,out}}} = \frac{\sum_{g=1}^{N_D}\left([P_j]_{N_{L,\,out}}\right)_g}{N_D} \quad (15)$$

$$M_n = \frac{\sum_j \overline{[P_j]_{N_{L,\,out}}} M_j}{\sum_j \overline{[P_j]_{N_{L,\,out}}}} \quad (16)$$

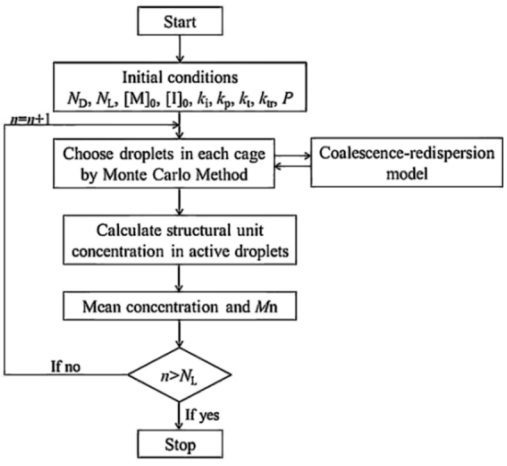


Figure 2. Simulation flow chart for the models.

According to the description of the experimental process and the input parameters in the modeling flow chart, the main influence factors of M_n are the polymerization temperature, the concentrations of reactants and the parameters of RPB; the effects of these three influence factors were systematically studied.

3. Results

3.1. Effect of T and Estimation of Reaction Rate Constant

The effect of T on the M_n of PIB is shown in Figure 3. It is obvious that M_n decreases with increasing T in the range of 267 K to 290 K. Moreover, the experimental results are consistent with simulated results. Here, T determined the values of rate constants and M_n. Based on Figures 3 and 4, it can be deduced that the reaction rate decreased with increasing T, and the activation energy of the IB polymerization was negative. This inference is coincident with a report of Thomas et al. [35]. It can be concluded that a higher temperature is beneficial to obtain PIB with a lower molecular weight. However, the content of exo-olefin terminals in PIB chains decreases from 94 to 79 mol% with increasing temperature from 267 K to 290 K; thus, a higher temperature results in a lower content of exo-olefin terminals in PIB chains, which is similar to the results reported in the literature [7]. At the reaction temperature of 283 K, HRPIB with M_n of 2550 g·mol^{-1} and exo-olefin terminal content of 85 mol% was obtained.

$$\ln k_P = \left(-\frac{E_a}{r} \oplus \frac{1}{T} + \ln k_0\right). \quad (17)$$

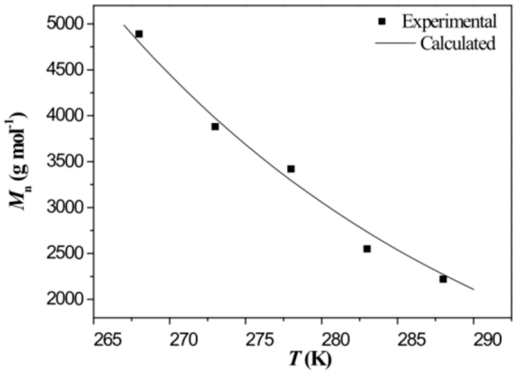


Figure 3. Effect of T on the M_n of PIB when Q_M = 33.7 L·h^{-1}, Q_I = 6.24 L·h^{-1}, $[M]_t$ = 2.00 mol·L^{-1}, $[I]_t$ = 0.22 mol·L^{-1} and N = 1600 rpm.

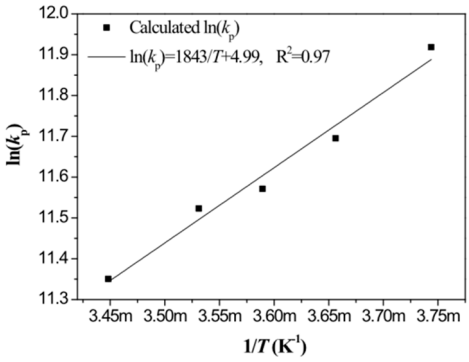


Figure 4. Arrhenius plot of lnk_p versus $1/T$ for the cationic polymerization of IB in RPB.

Based on the effect of T on the M_n of PIB and the developed models, the polymerization rate constant k_p was determined by the calculation flow chart shown in Figure 5. The results and corresponding T and experimental M_n are listed in Table 2. It can be seen in Table 2 that k_p decreases from about 10^4 to 10^5 L·mol^{-1}·s^{-1} with increasing T from 267 to 290 K, which is in the magnitude order range of $10^{5\pm1}$ L·mol^{-1}·s^{-1}, as reported previously [8,11,12]. From the linear fitting of lnk_p versus $1/T$ in Figure 4, according to the transformation of Arrhenius Equation (Equation (17)), the apparent activation energy E_a was −15.3 kJ·mol^{-1}. This E_a is within the generally accepted E_a range from −12.5 to −29 kJ·mol^{-1} for the cationic polymerization [36]. Furthermore, the k_i, k_{tr} and k_t under 283 K were respectively

calculated to be 10^4 L·mol^{-1}·s^{-1}, 10 L·mol^{-1}·s^{-1} and 10 s^{-1}, according to the flow chart in Figure 5. These kinetic parameters estimated from experimental data and modeling results fit well with previous reports such as $k_{tr}/k_p \approx 10^{-4}$ [37].

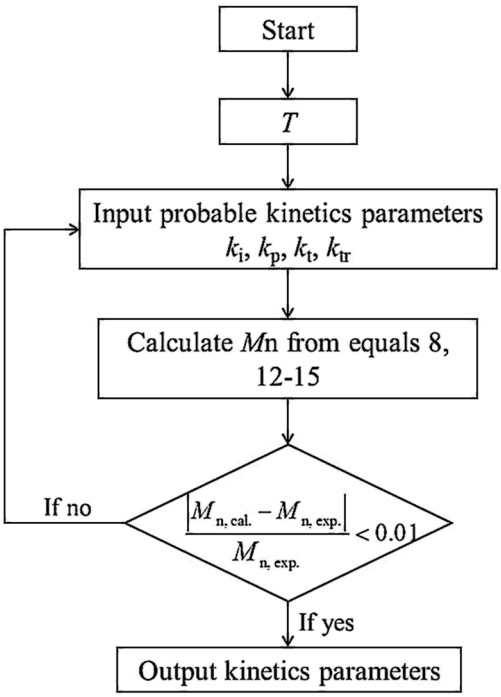


Figure 5. Calculation flow chart for the kinetic parameters.

Table 2. The calculated values of k_p based on T and experimental M_n.

T/K	M_n/(g·mol^{-1})	k_p/(10^4 L·mol^{-1}·s^{-1})
267	4890	15.0
274	3880	12.0
279	3420	10.6
283	2550	10.1
290	2220	8.5

[1] Q_M = 33.7 L·h^{-1}, Q_I = 6.24 L·h^{-1}, $[M]_t$ = 2.00 mol·L^{-1}, $[I]_t$ = 0.22 mol·L^{-1}, N = 1600 rpm.

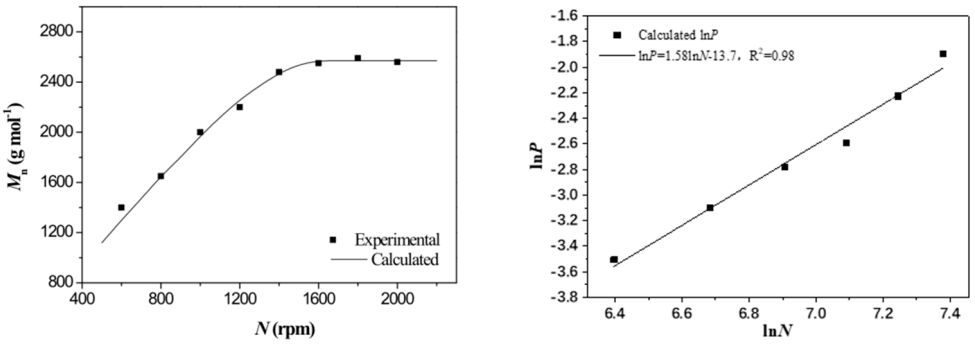
3.2. Effect of N and Estimation of P

The effect of the rotating speed N on the M_n of PIB is displayed in Figure 6a. It is observed that M_n increases remarkably from 1400 to 2550 g·mol^{-1} with increasing N from 600 to 1600 rpm, and then reaches a plateau when N is larger than 1600 rpm. The simulated M_n fits well with the experimental data. These results indicated that the polymerization of PIB could be intensified by enhancing the mixture in RPB, and the M_n could be tuned by regulating rotating speed. Moreover, both the micromixing rate and coalescence–redispersion frequency of the liquid droplets could be enhanced by increasing N [28,38]. The percentage of droplet number participating in coalescence–redispersion process is denoted by the coalescence probability P; it can be calculated with the analogous flow chart as shown in Figure 4 and listed in Table 3. It is observed that P increases with increasing N from 600 rpm to 1600 rpm. LnP is linearly related to ln$N$ when N is less than 1600 rpm, as shown in Figure 6b. The relationship between N and P is deduced as Equations (18) and (19), which is consistent with a previous report [17]. Moreover, exo-olefin terminal content in HRPIB is calculated as about 85 mol% and insensitive to

N, so M_n of HRPIB can be tuned by adjusting N from 0 to 1600 rpm without affecting exo-olefin terminal content.

$$P = 1.12 \times 10^{-6} \cdot N^{1.58}, \ (N \leq 1600 \text{ rpm}) \quad (18)$$

$$P = 0.15, \ (N > 1600 \text{ rpm}) \quad (19)$$



(**a**) (**b**)

Figure 6. (**a**) Effect of N on the M_n of PIB when Q_M = 33.7 L·h^{-1}, Q_I = 6.24 L·h^{-1}, $[M]_t$ = 2.00 mol·L^{-1}, $[I]_t$ = 0.22 mol·L^{-1} and T = 283 K. (**b**) Linear fitting of ln$P$ versus ln$N$ for cationic polymerization of IB in RPB.

Table 3. The calculated values of P based on N and experimental M_n.

N/rpm	M_n/(g·mol^{-1})	*P*
600	1400	0.030
800	1650	0.045
1000	2000	0.062
1200	2200	0.075
1400	2480	0.108
1600	2550	0.150
1800	2590	0.151
2000	2560	0.150

[1] Q_M = 33.7 L·h^{-1}, Q_I = 6.24 L·h^{-1}, $[M]_t$ = 2.00 mol·L^{-1}, $[I]_t$ = 0.22 mol·L^{-1}, N = 1600 rpm.

3.3. Effect of [M]$_0$/[I]$_0$

The effect of $[M]_0/[I]_0$ on the M_n of PIB is displayed in Figure 7, where $[M]_0/[I]_0$ is the initial concentration ratio of the monomer and initiating system in RPB. It is observed that M_n decreases with decreasing $[M]_0/[I]_0$ no matter whether $[M]_0/[I]_0$ is changed through decreasing $[M]_t$, decreasing Q_M, increasing $[I]_t$ or increasing Q_I. The simulated M_n fits well with the experimental M_n. The decrease in $[M]_0/[I]_0$ would reduce the relative quantity of monomers and improve the relative quantity of active centers, resulting in the decrease in M_n. It is worth noting that the effect of $[M]_0/[I]_0$ on the M_n in Figure 7a,c is more remarkable than that in Figure 7b,d, which indicates that M_n is more sensitive to changes in the monomer parameters. It can be concluded that M_n of PIB can be tuned by altering $[M]_t$, $[I]_t$, Q_M and Q_I, and a low $[M]_0/[I]_0$ is necessary to obtain low molecular weights of PIB. However, a low $[M]_0/[I]_0$ is detrimental to the content of exo-olefin terminals in PIB [6], since a decrease in exo-olefin terminal content from 92 to 78 mol% is observed with decreasing $[M]_0/[I]_0$ from 135 to 30. Therefore, a suitable $[M]_0/[I]_0$ should be chosen considering the demands of both the molecular weight and exo-olefin terminal content. In this paper, optimal $[M]_0/[I]_0$ was found to be 49, where HRPIB with M_n of 2550 g·mol^{-1} and exo-olefin terminal content of 85 mol% could be obtained.

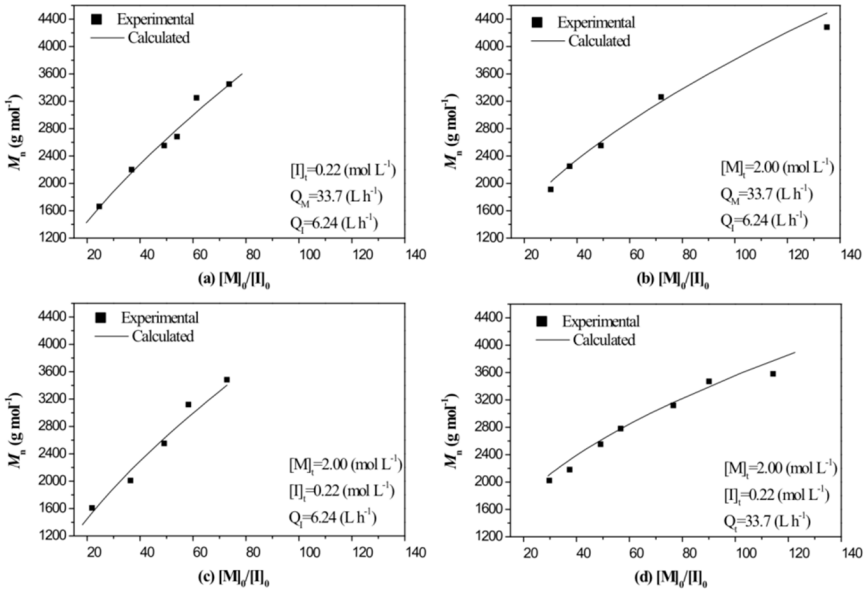


Figure 7. Effects of $[M]_0/[I]_0$ on the M_n of PIB when T = 283 K and N = 1600 rpm. The $[M]_0/[I]_0$ was changed by (**a**) changing $[M]_t$, (**b**) changing $[I]_t$, (**c**) changing Q_M and (**d**) changing Q_I.

3.4. Model Error Analysis

In the above discussions, the model based on the presumptive-steady-state analysis method and the coalescence–redispersion model was demonstrated as simulated M_n that fitted well with the experimental M_n. The diagonal plot of all simulated and experimental M_n at different T, N and $[M]_0/[I]_0$ is shown in Figure 8. It indicates that the model can offer predictions of the M_n of PIB synthesized in RPB, with a deviation within 10%. This 10% deviation from the experimental values could be regarded as a relative precision, which is similar to that of the mathematical model based on the chain analysis method and the coalescence–redispersion model [17].

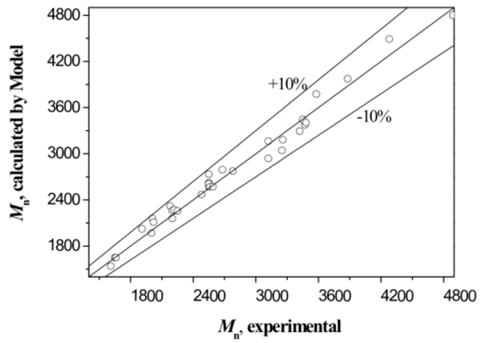


Figure 8. Comparison between experimental and modeling M_n.

4. Conclusions

With advantages related to its enhanced mixing effect, RPB was employed for the synthesis of HRPIB with low molecular weights. It was observed that M_n and exo-olefin terminal content in PIB both decreased with the increase in T and the decrease in $[M]_0/[I]_0$. When N was from 600 to 1600 rpm, M_n was from 1400 to 2550 g·mol^{-1}, but exo-olefin terminal content did not change. It was concluded that T, N, $[M]_t$, $[I]_t$, Q_M and Q_I could be used to regulate M_n of HRPIB, and optimal parameters for synthesizing HRPIB were determined as T of 283 K, N of 1600 rpm and $[M]_0/[I]_0$ of 49, where HRPIB with M_n of 2550 g·mol^{-1} and exo-olefin terminals content of 85 mol% was obtained. Our results demonstrate that RPB is a promising reactor for synthesizing HRPIB. Based on the presumptive-steady-state analysis method and the coalescence–redispersion model, a mathematical model was newly

presented to simulate the IB polymerization process in RPB and was used to predict M_n of HRPIB. The kinetic parameters of IB polymerization and the coalescence probability of droplets in the RPB were determined by the model. As a function of T, N and $[M]_0/[I]_0$, the simulated M_n fitted well with the experimental values, with a deviation within 10%. It is believed that this model can be widely applied for describing cationic polymerization processes in RPB.

Author Contributions: Methodology, W.W.; software, W.W. and W.H.; formal analysis, W.H.; investigation, W.H.; resources, Y.X., G.C., H.Z. and B.S.; writing—original draft preparation, W.H.; writing—review and editing, W.W., Y.X., Y.L. and B.S.; project administration, G.C. and B.S. All authors have read and agreed to the published version of the manuscript.

Funding: This research was funded by National Natural Science Foundation of China (Nos. 21725601, 21878009).

Acknowledgments: The Liu's lab.

Conflicts of Interest: The authors declare no conflict of interest.

Notation

T	polymerization temperature, K
N	rotating speed of rotator in RPB, rpm ($r \cdot min^{-1}$)
M_n	number-average molecular weight, $g \cdot mol^{-1}$
$[M]_t$	concentration of IB in tank, $mol \cdot L^{-1}$
$[M]_0$	initial concentration of IB in RPB, $mol \cdot L^{-1}$
$[M]$	concentration of IB in RPB, $mol \cdot L^{-1}$
$[I]_t$	concentration of initiating system in tank, $mol \cdot L^{-1}$
$[I]_0$	initial concentration of initiating system in RPB, $mol \cdot L^{-1}$
$[I]$	concentration of initiating system in RPB, $mol \cdot L^{-1}$
Q_M	volumetric flow rate of IB solution, $L \cdot h^{-1}$
Q_I	volumetric flow rate of initiating system solution, $L \cdot h^{-1}$
D	packing thickness in RPB, mm
N_L	total cage number of packing
N_D	droplets number in every cage
R_i	inner radius of rotator in RPB, mm
R_o	outer radius of rotator in RPB, mm
r_i	initiation rate, $mol \cdot L^{-1} \cdot s^{-1}$
r_p	propagation rate, $mol \cdot L^{-1} \cdot s^{-1}$
r_{tr}	chain transfer rate, $mol \cdot L^{-1} \cdot s^{-1}$
r_t	termination rate, $mol \cdot L^{-1} \cdot s^{-1}$
$\left[P_j^{\oplus}\right]$	concentration of active left, $mol \cdot L^{-1}$
$[P_j]$	concentration of polymer with j units, $mol \cdot L^{-1}$
$[P_j]_{N_{L,\,out}}$	concentration of polymer with j units out of packing, $mol \cdot L^{-1}$
k_i	rate constant for initiation, $L \cdot mol^{-1} \cdot s^{-1}$
k_p	rate constant for propagation, $L \cdot mol^{-1} \cdot s^{-1}$
k_{tr}	rate constant for chain transfer to monomer, $L \cdot mol^{-1} \cdot s^{-1}$
k_t	rate constant for termination, s^{-1}
M_j	56j molecular weight of polymer with j units, $g \cdot mol^{-1}$
t_m	micromixing characteristic time, ms
$t_{1/2}$	reactive characteristic time, ms
k_0	pre-exponential factor
R	molar gas constant, $J \cdot mol^{-1} \cdot K^{-1}$
E_a	apparent activation energy, $kJ \cdot mol^{-1}$
P	coalescence probability
Greek letters	
δ	distance between adjacent cages, mm

References

1. Liu, Q.; Wu, Y.X.; Yan, P.F.; Zhang, Y.; Xu, R.W. Polyisobutylene with High Exo-olefin Content via β-H Elimination in the Cationic Polymerization of Isobutylene with $H_2O/FeCl_3$/dialkyl ether Initiating System. *Macromolecules* **2011**, *44*, 1866–1875. [CrossRef]
2. Vasilenko, I.V.; Kostjuk, S.V. Homogeneous and heterogeneous catalysts for the synthesis of highly reactive polyisobutylene: Discovery, development and perspectives. *J. Macromol. Sci. Part A* **2021**, 1–11. [CrossRef]
3. Rajasekhar, T.; Singh, G.; Kapur, G.S.; Ramakumar, S.S.V. Recent Advances in Catalytic Chain Transfer Polymerization of Isobutylene: A Review. *RSC Adv.* **2020**, *10*, 18180–18191. [CrossRef]
4. Kostjuk, S.V. Recent Progress in the Lewis Acid Co-Initiated Cationic Polymerization of Isobutylene and 1,3-Dienes. *RSC Adv.* **2015**, *5*, 13125–13144. [CrossRef]
5. Li, Y.; Cokoja, M.; Kühn, F.E. Inorganic/Organometallic Catalysts and Initiators Involving Weakly Coordinating Anions for Isobutene Polymerisation. *Coord. Chem. Rev.* **2011**, *255*, 1541–1557.
6. Kostjuk, S.V.; Yeong, H.Y.; Voit, B. Cationic Polymerization of Isobutylene at Room Temperature. *J. Polym. Sci. A Polym. Chem.* **2013**, *51*, 471–486. [CrossRef]
7. Liu, Q.; Wu, Y.X.; Zhang, Y.; Yan, P.F.; Xu, R.W. A cost-effective process for highly reactive polyisobutylenes via cationic polymerization coinitiated by AlCl3. *Polymer* **2010**, *51*, 5960–5969. [CrossRef]
8. Sigwalt, P.; Moreau, M. Carbocationic Polymerization: Mechanisms and Kinetics of Propagation Reactions. *Prog. Polym. Sci.* **2006**, *31*, 44–120. [CrossRef]
9. Matyjaszewski, K.; Pugh, C. Mechanistic aspects of cationic polymerization of alkenes. In *Cationic Polymerization: Mechanisms, Synthesis, and Applications*; Dekker M Press: New York, NY, USA, 1996; pp. 192–204.
10. Qiu, Y.X.; Wu, Y.X.; Xu, X.; Ran, F.; Wu, G.Y. Propagation Rate Constants for the Cationic Polymerization of Vinyl Monomer. *Chin. Polym. Bull.* **2006**, *4*, 1–10.
11. Plesch, P.H. The Propagation Rate Constants of the Cationic Polymerization of Alkenes. *Prog. React. Kinet.* **1993**, *18*, 1–62.
12. Puskas, J.E.; Shaikh, S.; Yao, K.Z.; McAuley, K.B.; Kaszas, G. Kinetic Simulation of Living Carbocationic Polymerizations. II. Simulation of Living Isobutylene Polymerization using a mechanistic model. *Eur. Polym. J.* **2005**, *41*, 1–14. [CrossRef]
13. Wu, G.Y.; Wu, Y.X. *Controlling Cationic Polymerization and Its Application*; Chem. Ind. Press: Beijing, China, 2005.
14. Liu, D.H. *Handbook of Synthetic Rubber Industry*; Chem. Ind. Press: Beijing, China, 1991.
15. Kennedy, J.P.; Macrechal, E. *Carbocationic Polymerization*; Wiley: New York, NY, USA, 1982.
16. Chen, G.T. *Foundation of Polymer Reactive Engineering*; China Petrochemical Press: Beijing, China, 1991.
17. Chen, J.F.; Gao, H.; Zou, H.K.; Chu, G.W.; Zhang, L.; Shao, L.; Xiang, Y.; Wu, Y.X. Cationic Polymerization in Rotating Packed Bed Reactor: Experimental and Modeling. *AIChE J.* **2010**, *56*, 1053–1062. [CrossRef]
18. Chen, J.F.; Wang, Y.H.; Guo, F.; Wang, X.M.; Zheng, C. Synthesis of Nanoparticles with Novel Technology: High-gravity Reactive Precipitation. *Ind. Eng. Chem. Res.* **2000**, *39*, 948–954. [CrossRef]
19. Munjal, S.; Dudukovc, M.P.; Ramachandran, P. Mass Transfer in Rotating Packed Beds-I. Development of Gas-liquid and Liquid-solid Mass-transfer Correlations. *Chem. Eng. Sci.* **1989**, *44*, 2245–2256. [CrossRef]
20. Ramshaw, C.; Mallinson, R. Mass Transfer Process. U.S. Patent 4,263,255, 11 August 1981.
21. Chen, J.F. *High Gravity Technology and Application-a New Generation of Reaction and Separation Technology*; Chem. Ind. Press: Beijing, China, 2003. (In Chinese)
22. Chen, J.F.; Shao, L.; Guo, F.; Wang, X.M. Synthesis of Nano-fibers of Aluminum Hydroxide in Novel Rotating Packed Bed Reactor. *Chem. Eng. Sci.* **2003**, *58*, 569–575. [CrossRef]
23. Wang, M.; Zou, H.K.; Shao, L.; Chen, J.F. Controlling Factors and Mechanism of Preparing Needlelike $CaCO_3$ under High-gravity Environment. *Powder Technol.* **2004**, *142*, 166–174. [CrossRef]
24. Chen, J.F.; Shao, L. Mass Production of Nanoparticles by High Gravity Reactive Precipitation Technology with Low Cost. *China Particuology* **2003**, *1*, 64–69. [CrossRef]
25. Guo, K.; Guo, F.; Feng, Y.D.; Chen, J.F.; Zheng, C.; Gardner, N.C. Synchronous Visual and RTD Study on Liquid Flow in Rotating Packed Bed Contactor. *Chem. Eng. Sci.* **2000**, *55*, 1699–1706. [CrossRef]
26. Chen, J.F.; Zhou, M.Y.; Shao, L.; Wang, Y.Y.; Yun, J.; Chew, N.Y.K.; Chan, H.K. Feasibility of Preparing Nanodrugs by High-gravity Reactive Precipitation. *Int. J. Pharm.* **2004**, *269*, 267–274. [CrossRef]
27. Chen, Y.H.; Chang, C.Y.; Su, W.L.; Chen, C.C.; Chiu, C.Y.; Yu, Y.H.; Chiang, P.C.; Chiang, S.I.M. Modeling Ozone Contacting Process in a Rotating Packed Bed. *Ind. Eng. Chem. Res.* **2004**, *43*, 228–236. [CrossRef]
28. Yang, H.J.; Chu, G.W.; Zhang, J.W.; Shen, Z.G.; Chen, J.F. Micromixing Efficiency in a Rotating Packed Bed: Experiments and Simulation. *Ind. Eng. Chem. Res.* **2005**, *44*, 7730–7737. [CrossRef]
29. Chen, J.F.; Gao, H.; Wu, Y.X.; Zou, H.K.; Chu, G.W.; Zhang, L. Method for Synthesis of Butyl Rubber. U.S. Patent 12,307,121, 17 August 2010.
30. Curl, R.L. Disperse Phase Mixing I: Theory and Effects in Simple Reactors. *AIChE J.* **1963**, *9*, 175–181. [CrossRef]
31. Chen, G.T. Kinetic Models of Homogeneous Ionic Polymerization. *J. Polym. Sci. Pol. Chem. Edit.* **1982**, *20*, 2915–2934. [CrossRef]
32. Wu, G.; Wu, Y. *Control Cationic Polymerization and Its Application*; Chemical Industry Press: Beijing, China, 2004; pp. 166–173.
33. Wang, J.D. Real-time Dynamic Simulation of Low Density Polyethylene Reactor under High Pressure. Master's Thesis, Beijing University of Chemical Technology, Beijing, China, 1997.

34. Wang, W.S.; Li, S.F. Conditional Contractivity of Runge-Kutta Methods for Nonlinear Differential Equations with Many Variable Delays. *Commun. Nonlinear Sci. Numer. Simul.* **2009**, *14*, 399–408. [CrossRef]
35. Thomas, Q.A.; Storey, R.F. Effect of Reaction Conditions on Apparent TiCl4 Reaction Order in Quasiliving Isobutylene Polymerization at High [initiator]/[$TiCl_4$] Ratios. *Macromolecules* **2003**, *36*, 10120–10125. [CrossRef]
36. Pan, Z.R. *Polymer Chemistry*; Chem. Ind. Press: Beijing, China, 2002.
37. Fordor, Z.; Bae, Y.C.; Faust, R. Temperature Effects on the Living Cationic Polymerization of Isobutylene: Determination of Spontaneous Chain-transfer Constants in the Presence of Terminative Chain Transfer. *Macromolecules* **1998**, *31*, 4439–4446. [CrossRef]
38. Yang, H.J.; Chu, G.W.; Xiang, Y.; Chen, J.F. Characterization of Micro-mixing Efficiency in Rotating Packed Beds by Chemical Methods. *Chem. Eng. J.* **2006**, *121*, 147–152. [CrossRef]